Efficient photoemission and ionization of He^+ by a combined fundamental laser and high-order harmonic pulse

Kenichi L. Ishikawa*
Department of Quantum Engineering and Systems Science, Graduate School of Engineering, University of Tokyo, Hongo 7-3-1, Bunkyo-ku, Tokyo 113-8656, Japan
(Received 14 January 2004; revised manuscript received 8 April 2004; published 28 July 2004)

We theoretically study the behavior of He^+ exposed simultaneously to an ultrashort intense Ti:sapphire laser and its 27th or 13th harmonic pulses, by solving the time-dependent Schrödinger equation using the alternating direction implicit method. This system is chosen as an interesting application of state-of-the-art high-order harmonic sources. Our results show that the simple hydrogenlike system exhibits surprising responses. The addition of the 27th harmonic enhances high-order harmonic photoemission from He^+ even by 17 orders of magnitude compared with the case of the fundamental pulse alone, i.e., usual high-order harmonic generation, and the H13 addition also increases photoemission efficiency by more than ten orders of magnitude. Moreover, while an individual 10 fs laser (wavelength $\lambda_F = 800$ nm) or its 27th harmonic pulse with a peak intensity of 3×10^{14} and 10^{13} W/cm^2, respectively, ionizes no more than 5×10^{-6} of He^+, their combined pulse leads to a much higher He^{2+} yield of 17%. The photoemission efficiency only weakly depends on the fundamental wavelength, and the main plateau efficiency scales as the intensity of the 27th harmonic pulse. The He^{2+} yield is linear in the intensity of the 27th harmonic and quadratic in that of the 13th harmonic pulse. Its dependence on fundamental intensity is much more complex, even containing a range where the yield decreases with increasing laser intensity, due to the dynamic Stark effect. Detailed analyses reveal that the mechanism of the enhancement of harmonic photoemission as well as ionization is a combination of harmonic generation from a coherent superposition of states and two-color frequency mixing enhanced by the presence of a near-resonant intermediate level, and that their relative importance depends on fundamental wavelength.

DOI: 10.1103/PhysRevA.70.013412 PACS number(s): 32.80.Rm, 42.50.Hz, 42.65.Ky

I. INTRODUCTION

Since the advent of ultrashort high-peak-power lasers, many interesting phenomena of high-field physics have become available for application. In particular, high-order harmonic generation (HHG) [1,2] can produce ultrashort coherent soft x-ray and extreme ultraviolet (xuv) pulses from a compact laser system. Moreover, recent progress in the phase-matching technique by use of a long interaction medium has enabled the production of high-power soft x-ray and xuv pulses [3–10]. Takahashi *et al.* [3] have succeeded in the generation of the 27th harmonic pulses (wavelength $\lambda_H = 29.6$ nm) of a Ti:sapphire laser with a pulse width smaller than 30 fs and an output energy of 0.33 μJ per pulse. The same authors have subsequently reported the generation of 11th, 13th and 15th harmonic pulses ($\lambda_H = 72.7$, 62.3, and 54 nm) with an output energy as high as 7, 4.7, and 1 μJ, respectively [4], and that of 59th harmonic pulses ($\lambda_H = 13.5$ nm) with an output energy of 25 nJ/pulse [8]. Hergott *et al.* [9] has generated 15th harmonic pulses ($\lambda_H = 53.3$ nm) of a Ti:sapphire laser with an energy of 1.9 μJ per pulse, while Yoshitomi *et al.* [10] has recently generated 5th harmonic pulses ($\lambda_H = 50$ nm) of a KrF excimer laser with an energy of 1.2 μJ. When these harmonic pulses are focused to an area of 10 μm^2 using a mirror, its average intensity can reach 10^{14} W/cm^2 in the soft x-ray and 10^{15} W/cm^2 in the xuv domain [11,12].

With such relatively simple but intense light sources at hand, a variety of applications such as ultrafast xuv holography, the diagnosis of dense bright plasmas, and even the study of nonlinear optical processes in the xuv and soft x-ray ranges, limited so far to a longer wavelength [13–15], might become possible. In this context, Ishikawa and Midorikawa [16] have proposed two-photon ionization of He^+ by Ti:sapphire 27th harmonic (H27) pulses as a candidate for the experimental observation of a nonlinear optical effect in the soft x-ray domain, and Nakajima and Nikolopoulos [17] have theoretically shown that the two-photon double ionization of He may be observed with the same harmonic. Moreover, several applications of the high-order harmonics (HH) have recently been demonstrated in solid-state and plasma physics [18], and Hentschel *et al.* [19] have demonstrated the measurement of attosecond pulse duration using a HH.

In the present paper, we theoretically study the response of a He^+ ion subject to a fundamental Ti:sapphire laser pulse and an intense 27th or 13th harmonic pulse at the same time, as an application of state-of-the-art HH sources. It is true that there exist studies on the behavior of a hydrogen atom [20–22] and a one-dimensional model atom [23] irradiated simultaneously by a fundamental and its harmonic (H3 [20], H7 [21], and H11 [22,23]) pulses. It should be noted, however, that due to its high ionization potential (54.4 eV) He^+ may be applied to generate harmonics of higher orders than possible today and is not ionized by a single H27 and H13 photon, for which high-power pulses are available, in contrast to a hydrogen atom. In the present study, we are interested especially in the effects of the simultaneous irradiation

*Electronic address: ishiken@q.t.u-tokyo.ac.jp

on harmonic photoemission and ionization. The fundamental laser pulse can hardly ionize He^+ as we will see later. Although thanks to high ionization potential the harmonic spectrum from this ion would have higher cutoff energy than in the case of commonly used rare-gas atoms [3–10], the conversion efficiency is extremely low due to the small ionization probability. It is, however, noteworthy that the H27 photon energy and twice the H13 photon energy happen to be close to resonance, though not exactly, with a transition to the $2p$ or $2s$ levels from the ground state. It is expected, therefore, that the addition of a Ti:sapphire 27th or 13th harmonic pulse can totally change the behavior of the He^+ ion under an intense laser field.

We solve numerically the time-dependent Schrödinger equation (TDSE) for He^+ interacting with a combined ultrashort intense laser and its 27th or 13th harmonic pulse, using the alternating direction implicit method [24]. Our results show that the combination of fundamental laser and its 27th or 13th harmonic pulses enhance both high-order harmonic generation and ionization by more than ten orders of magnitude [25,26]. For example, photoemission efficiency by a combined 10 fs laser (wavelength $\lambda_F = 800$ nm) and its 27th harmonic pulse with a peak intensity of 3×10^{14} and 10^{13} W/cm^2, respectively, is by 17 orders of magnitude higher than in the case of the laser pulse alone. This is by far more dramatic than previously reported moderate enhancement [20,23,27]. According to our detailed analyses, the enhancement is due to a combination of harmonic generation from a coherent superposition of states and two-color frequency mixing enhanced by the presence of a near-resonant intermediate level, and their relative importance depends on the fundamental wavelength.

The present paper is organized as follows. In Sec. II we briefly summarize the simulation model. In Sec. III we apply the model to the calculation of photoemission and ionization of He^+ under the simultaneous irradiation of a fundamental laser and its 27th of 13th harmonic pulses and examine their dependence on intensity and wavelength. In Sec. IV we analyze the mechanism of photoemission and ionization enhancement, starting from the wavelength dependence of the He^{2+} yield. The conclusions are given in Sec. V.

II. MODEL

To study the interaction of a He^+ ion with a combined laser and harmonic pulse, we solve the time-dependent Schrödinger equation in the length gauge,

$$i\frac{\partial\Phi(\mathbf{r},t)}{\partial t} = \left[-\frac{1}{2}\nabla^2 - \frac{2}{r} - zE(t)\right]\Phi(\mathbf{r},t), \qquad (1)$$

where $E(t)$ is the electric field of the pulse. Here we have assumed that the field is linearly polarized in the z-direction. Equation (1) is numerically integrated using the alternating direction implicit (Peaceman-Rachford) method [24]. To reduce the difference between the discretized and analytical wave function, we scale the Coulomb potential by a few percent at the first grid point [28]. To prevent reflection of the wave function from the grid boundary, after each time step the wave function is multiplied by a $\cos^{1/8}$ mask function [28] that varies from 1 to 0 over a width of 2/9 of the maximum radius at the outer radial boundary. The ionization yield is evaluated as the decrease of the norm of the wave function on the grid, and the photoemission spectrum is obtained from the Fourier transform of the dipole acceleration.

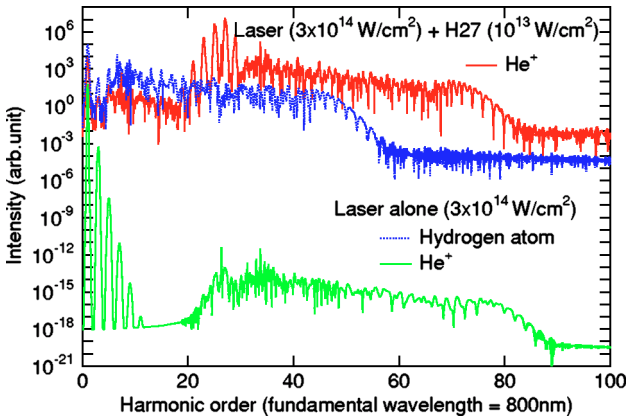

FIG. 1. (Color online) Upper solid curve: harmonic spectrum from He^+ exposed to a Gaussian combined fundamental and its 27th harmonic pulse with a duration (FWHM) of 10 fs, the former with a peak intensity of 3×10^{14} W/cm^2 and the latter 10^{13} W/cm^2. The fundamental wavelength is 800 nm. Lower solid and dotted curves: harmonic spectrum from He^+ and a hydrogen atom, respectively, exposed to the fundamental pulse alone. Nearly straight lines beyond the cutoff energy are due to numerical noise.

The electric field $E(t)$ is assumed to be given by

$$E(t) = F_F(t)\sin(\omega t) + F_H(t)\sin(n\omega t + \phi), \qquad (2)$$

with $F_F(t)$ and $F_H(t)$ being the pulse envelope of the fundamental and harmonic pulse, respectively, chosen to be Gaussian with a duration (full width at half maximum) of 10 fs, ω the angular frequency of the fundamental pulse, n the harmonic order, and ϕ the relative phase. In typical calculations, we use a grid with a maximum radius of 125–250 a.u. and maximum number of partial waves $L_{max} = 100-200$. The grid spacing is 0.125 a.u., and the time step is 1/65536 of an optical cycle t_L of the Ti:sapphire laser light.

We have also solved Eq. (1) using a method elaborated based on an explicit finite difference scheme for several cases and confirmed that the results remain virtually the same as those obtained with the Peaceman-Rachford method.

III. PHOTOEMISSION AND IONIZATION ENHANCEMENT

In this section, we study how the harmonic photoemission and ionization behavior of a He^+ ion is affected by the addition of an intense 27th or 13th harmonic pulse and how they depend on the phase, wavelength, and intensity of the pulse.

A. Photoemission

In Fig. 1 we show the harmonic photoemission spectrum from He^+ for the case of simultaneous fundamental and H27 irradiation. The fundamental wavelength λ_F is 800 nm, the peak fundamental intensity I_F is 3×10^{14} W/cm^2, and the

peak H27 intensity I_{H27} is 10^{13} W/cm^2. For comparison we also show the spectra obtained when only the fundamental pulse of the same intensity is applied to a He^+ ion and a hydrogen atom. The general feature of HHG can be explained by the classical model, which is usually called the *simpleman's theory* or three-step model [29]. According to this model, an electron is lifted to the continuum at the nuclear position with no kinetic energy, the subsequent motion is governed classically by an oscillating electric field, and a harmonic is emitted upon recombination. As a result, the highest harmonic (the cutoff) has an energy E_c given by [29]

$$E_c = I_p + 3.17U_p, \tag{3}$$

where I_p and U_p are the ionization potential and the ponderomotive energy, respectively. This equation tells us that a way of getting higher harmonics is to use an atom or an ion with a larger ionization potential. For the case of Fig. 1, the cutoff energy is calculated from Eq. (3) to be 70 eV (H45) for a hydrogen atom and 111 eV (H72) for a He^+ ion. The cutoff positions in Fig. 1 roughly agree with these values, though the cutoff for He^+ is somewhat higher than predicted by the simpleman's theory, which is because the distance between the nuclear position and the appearance position of the electron is not negligible, as is discussed in Ref. [30]. As a result, harmonics of much higher orders are generated from He^+ than from H. We note, however, that the harmonic intensity from He^+ when only the laser is applied is extremely low compared with the case of H. This is because the large ionization potential, though advantageous in terms of the cutoff energy, hinders the first step of the simpleman's theory, i.e., ionization.

The situation changes completely if the H27 pulse is simultaneously applied to He^+. From Fig. 1 we can see that the conversion efficiency is enhanced by about seventeen orders of magnitude. Moreover, the advantage of high cutoff is preserved, though its position is now closer to the value predicted by Eq. (3). Figure 2 shows the harmonic photoemission spectrum from He^+ for the case of simultaneous fundamental and H13 irradiation. Again the harmonic intensity is enhanced by more than ten orders of magnitude compared to the case of the laser pulse alone.

In order to examine the influence of the relative phase ϕ on photoemission, we have calculated spectra from He^+ subject to a combined fundamental and H27 pulse by varying the value of ϕ. Figure 3 compares the results for $\phi=0$ and $\phi=\pi/2$. The two curves are virtually indistinguishable. This may come as a surprise, since it is known that the detailed structure of a harmonic spectrum and ionization rate by a two-color field (typically, the fundamental and a few order harmonic field) depend on the relative phase [31–35]. In the case of the present study, the H27 field has too small a ponderomotive energy to participate in the second step of the simpleman's theory, i.e., classical acceleration of the ejected electron. Moreover, as we will see in Sec. IV, ionization is largely dominated by the path involving a single H27 photon and tunneling by the fundamental field, which renders the interference [33–35] of different ionization paths negligible. Therefore, the response of He^+ is insensitive to the relative

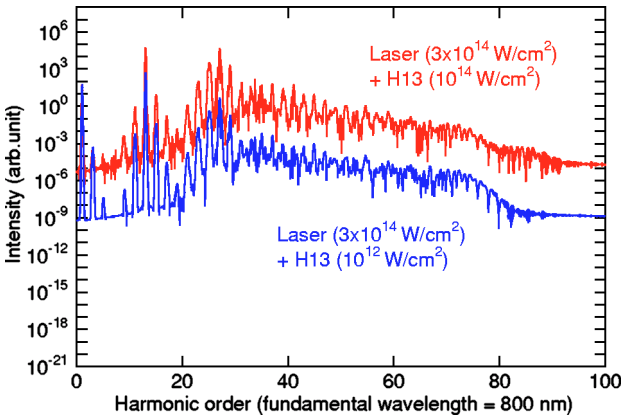

FIG. 2. (Color online) Harmonic spectrum from He^+ exposed to a Gaussian combined fundamental and its 13th harmonic pulse with a duration (FWHM) of 10 fs, the former with a peak intensity of 3×10^{14} W/cm^2, and the latter 10^{14} W/cm^2 (upper curve) and 10^{12} W/cm^2 (lower curve). The fundamental wavelength is 800 nm. Note that the horizontal axis is of the same scale as in Fig. 1.

phase between the fundamental and H27 pulses. We have found that this is also the case for a combined fundamental and H13 pulse, and that the results do not depend on the absolute phase of the pulse, either. Therefore, we set $\phi=0$ in the rest of the present paper.

In Fig. 4 we compare harmonic spectra from He^+ irradiated by a combined fundamental and H27 pulse with $\lambda_F=785$ nm and 800 nm. This figure shows that the harmonic intensity does not depend much on fundamental wavelength. We have varied λ_F between 750 and 850 nm and found a similar enhancement over the entire range. This result indi-

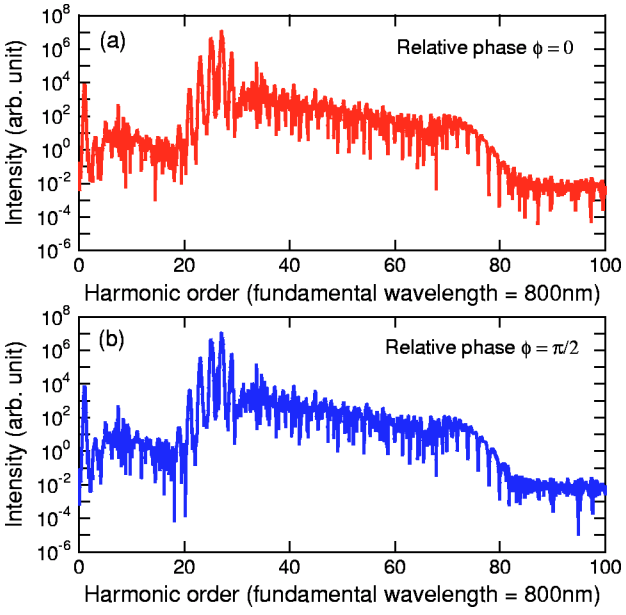

FIG. 3. (Color online) Harmonic spectra from He^+ subject to a combined fundamental and its 27th harmonic pulse with a duration (FWHM) of 10 fs and a relative phase of (a) $\phi=0$ and (b) $\phi=\pi/2$. The peak intensities and the fundamental wavelength are the same as in Fig. 1.

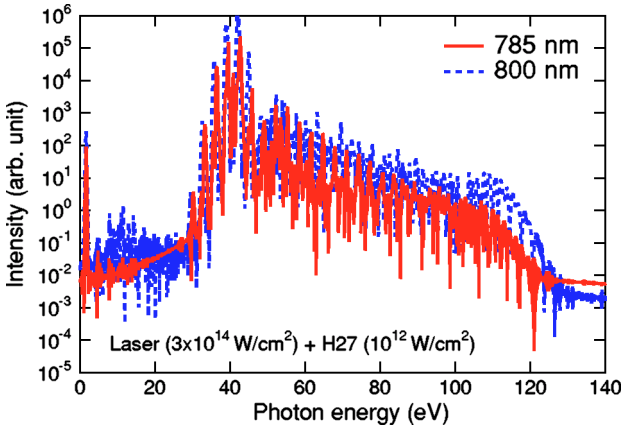

FIG. 4. (Color online) Harmonic spectra from He^+ exposed to a combined fundamental and its 27th harmonic pulse, the former with a peak intensity of 3×10^{14} W/cm^2 and the latter 10^{12} W/cm^2. The fundamental wavelength is 785 nm (solid curve) and 800 nm (dashed curve), respectively.

cates that fine tuning of the fundamental wavelength is not necessary for the enhancement of high-order harmonic photoemission. It should be noted in Fig. 4, however, that the two spectra are quite different in shape at a photon energy lower than 25 eV. The spectrum for $\lambda_F=800$ nm contains a small plateau in this range. On the other hand, for the case of $\lambda_F=785$ nm, the harmonic intensity decreases as a photon energy or harmonic order increases, and is lower than the numerical noise level at an energy between 15 and 25 eV. These observations suggest that the mechanism of photoemission enhancement depends on the fundamental wavelength, as we will discuss in Sec. IV.

Let us next examine the dependence of the photoemission spectra on the intensity of a H27 or H13 pulse. Figure 5 shows the ratio between the spectra from He^+ subject to a combined fundamental and H27 pulse for a peak H27 intensity I_{H27} of 10^{11} W/cm^2 and 10^{12} W/cm^2. The fundamental wavelength λ_F is 800 nm, and the peak fundamental intensity I_F is 3×10^{14} W/cm^2, as in Fig. 1. We can see that the

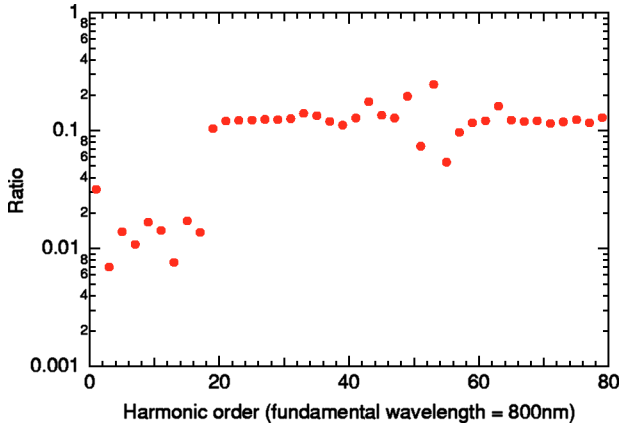

FIG. 5. (Color online) Ratio between the spectra at each odd harmonic frequency from He^+ subject to a combined fundamental and H27 pulse with a peak H27 intensity of 10^{11} W/cm^2 and 10^{12} W/cm^2. $\lambda_F=800$ nm and $I_F=3\times10^{14}$ W/cm^2.

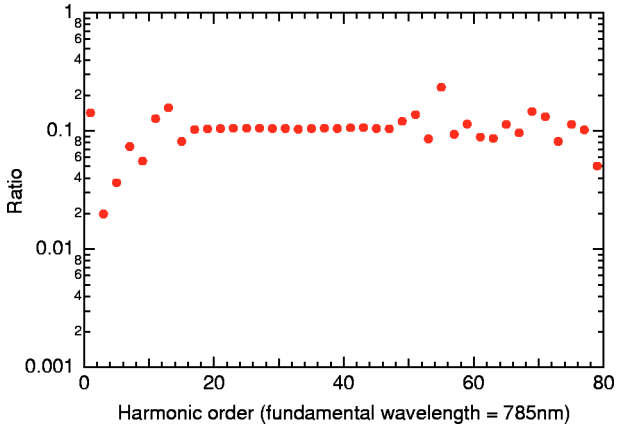

FIG. 6. (Color online) Ratio between the spectra at each odd harmonic frequency from He^+ subject to a combined fundamental and H27 pulse with a peak H27 intensity of 10^{11} W/cm^2 and 10^{12} W/cm^2. $\lambda_F=785$ nm and $I_F=3\times10^{14}$ W/cm^2.

ratio is abount 0.01 at harmonic orders lower than 15 (the first or small plateau) and about 0.1 at harmonic orders higher than 19 (the second or main plateau). This indicates that the spectral intensity is proportional to I_{H27}^2 at the small plateau while it is linear in I_{H27} at the main plateau at $\lambda_F=800$ nm. Figure 6 shows a similar ratio as in Fig. 5 for a fundamental wavelength of 785 nm. From Fig. 6 we can see that the spectral intensity is again linear in I_{H27} at the main plateau. On the other hand, at harmonic orders lower than 15, the dependence of spectral intensity on I_{H27} is not clear, partly because the intensity is close to the numerical noise level in this range.

B. Ionization

Let us now turn to ionization probability. Table I summarizes the He^{2+} yield for each case of the fundamental pulse alone, the harmonic pulse alone, and the combined pulse. The fundamental wavelength is 800 nm. Like harmonic photoemission spectra, the ionization probability by the combined pulse is also by more than ten orders of magnitude higher than that by the fundamental laser pulse alone. Especially strong enhancement is found in the case of the combined fundamental and H27 pulses: the He^{2+} yield is increased by several orders of magnitude also with respect to the case of the H27 irradiation alone. In Fig. 7, we plot the

TABLE I. The He^{2+} yield for various combinations of a Gaussian fundamental and its 27th or 13th harmonic pulses with a duration (FWHM) of 10 fs and a peak intensity listed in the table. $\lambda_F=800$ nm.

I_F (W/cm^2)	I_{H27} (W/cm^2)	I_{H13} (W/cm^2)	He^{2+} yield
3×10^{14}	–	–	2.29×10^{-15}
–	10^{13}	–	4.79×10^{-6}
3×10^{14}	10^{13}	–	0.173
–	–	10^{14}	1.25×10^{-4}
3×10^{14}	–	10^{14}	2.04×10^{-4}

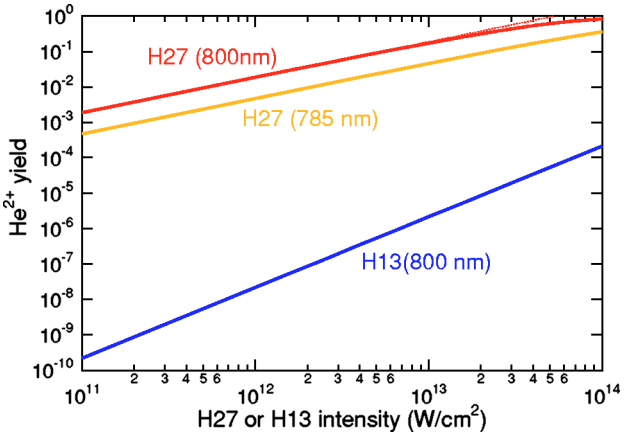

FIG. 7. (Color online) The He^{2+} yield as a function of peak intensity of the 27th (upper curve for $\lambda_F=800$ nm and middle for $\lambda_F=785$ nm) and 13th (lower curve for $\lambda_F=800$ nm) harmonic pulse when He^+ is exposed to a Gaussian combined fundamental and its 27th harmonic pulse with a duration (FWHM) of 10 fs. The peak intensity of the fundamental pulse is 3×10^{14} W/cm^2.

He^{2+} yield as a function of I_{H27} and I_{H13} for a fixed fundamental intensity of 3×10^{14} W/cm^2. Both for $\lambda_F=800$ nm and 785 nm, the ionization probability is linear in I_{H27} and quadratic in I_{H13} except for the saturation at $I_{H27}>10^{13}$ W/cm^2 for $\lambda_F=800$ nm, where the He^{2+} yield approaches unity. The dependence on I_{H27} and I_{H13} shown in Fig. 7 indicates that ionization process involves a single H27 photon or two H13 photons.

The variation of ionization with the peak intensity I_F of the fundamental pulse is much more complex than that with I_{H27} and I_{H13}. Figure 8 shows the dependence of the He^{2+} yield on I_F. For the case of a combined fundamental and H27 pulse with a fundamental wavelength of 800 nm, the yield hardly depends on I_F at laser intensity lower than 3×10^{12} W/cm^2. In this region, two-H27-photon ionization is

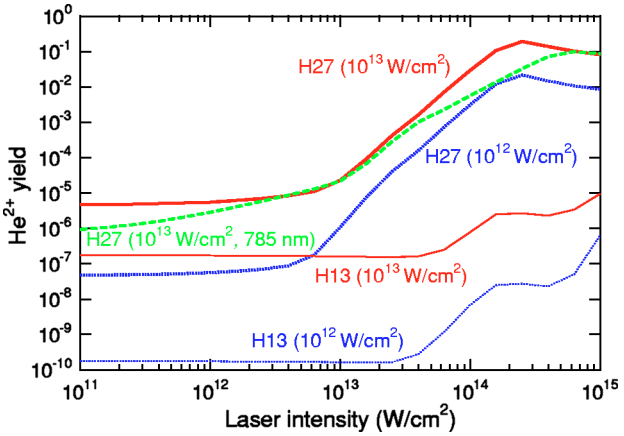

FIG. 8. (Color online) The He^{2+} yield as a function of peak intensity I_F of the fundamental laser pulse when He^+ is exposed to a Gaussian combined fundamental and its 27th or 13th harmonic pulse with a duration (FWHM) of 10 fs. The fundamental wavelength λ_F is 800 nm except for the dashed line, for which $\lambda_F=785$ nm. The peak intensity of each harmonic pulse is indicated in the figure along with its order.

dominant, which is supported by the fact that the yield is quadratic in H27 intensity and approximately equal to the value for the case where only a H27 pulse of the same intensity is applied (see Table I). At a laser intensity range between 3×10^{12} and 2×10^{14} W/cm^2, the He^{2+} yield rises rapidly with increasing laser intensity, indicating that the laser optical field plays an important role in ionization. It should be noted that the He^{2+} yield is proportional to peak H27 intensity in this range and at higher laser intensity. This suggests that a single H27 photon is involved in the ionization process there, as we have already discussed in Fig. 7. The results for a combined fundamental and H13 pulse with $\lambda_F=800$ nm can be interpreted in a similar fashion. In the case of a combined fundamental and H27 pulse with $\lambda_F=785$ nm, no region where the yield is nearly independent of I_F appears in the figure, since the yield of two-H27-photon ionization is relatively low (7.28×10^{-7}). What is surprising is, however, that the yield is not monotonically increasing in I_F: ionization is decreased with an increasing laser intensity at $I_F>3\times10^{14}$ W/cm^2 ($\lambda_F=800$ nm) and $I_F>6\times10^{14}$ W/cm^2 ($\lambda_F=785$ nm) in the presence of the H27 pulse and at $2\times10^{14}<I_F<4\times10^{14}$ W/cm^2 ($\lambda_F=800$ nm) in the presence of the H13 pulse. We will discuss the origin of this counter-intuitive behavior in the next section.

IV. ENHANCEMENT MECHANISM

In this section we explore in detail the underlying mechanism of the enhancement effects observed both in harmonic photoemission (Figs. 1 and 2) and in ionization (Table I), by far stronger than previously reported moderate enhancement [20,23,27]. Let us start with an analysis of the results presented in Fig. 8, in which the He^{2+} yield decreases with an increasing laser intensity in a certain range of I_F. In order to clarify the origin of this counter-intuitive behavior, we have calculated the dependence of the He^{2+} yield on the fundamental wavelength λ_F for different values of fundamental intensity. The results are shown in Fig. 9 for the cases of $I_{H27}=10^{13}$ W/cm^2 and $I_F=5\times10^{13}$, 8×10^{13}, 3×10^{14}, 5×10^{14}, 10^{15} W/cm^2.

The curve for $I_F=5\times10^{13}$ W/cm^2 peaks around $\lambda_F=820$ nm. Since the corresponding photon energy $\hbar\omega$ is 1.51 eV, the H27 photon energy ($27\hbar\omega=40.8$ eV) is exactly resonant with the $1s$-$2p$ transition. Thus, in this case, the electron is resonantly excited to the $2p$ state by a single H27 photon and is subsequently lifted to the continuum through optical field ionization (OFI) by a laser field. At $I_F=8\times10^{13}$ W/cm^2 we can see a second peak around $\lambda_F=793$ nm ($\hbar\omega=1.56$ eV), for which $26\hbar\omega$ ($=27\hbar\omega-\hbar\omega$) coincides with the $1s-2s$ transition energy. This indicates that at this wavelength the $2s$ level is resonantly populated through two-color two-photon excitation which involves single H27 and fundamental photons. With increasing laser intensity, the peaks are shifted to longer wavelengths due to the laser-induced dynamic Stark effect; the red shift is consistent with a standard formula for the effect [37].

At $I_F=3\times10^{14}$ W/cm^2, the second peak is now higher than the first one and is located around 800 nm. In Fig. 10 we show a temporal evolution of the $2s$ and $2p$ population of

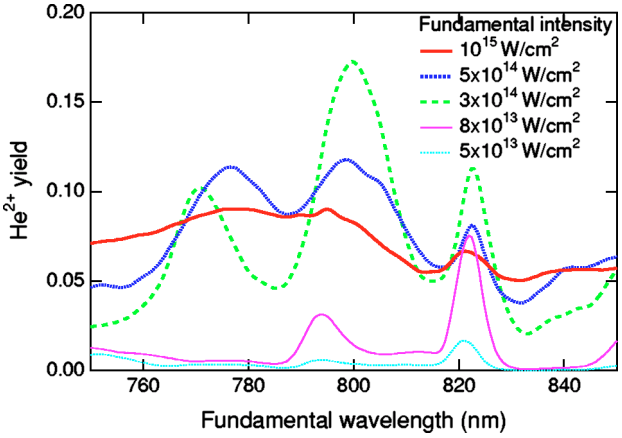

FIG. 9. (Color online) The He^{2+} yield as a function of fundamental wavelength when He^+ is exposed to a Gaussian combined fundamental and its 27th harmonic pulse with a duration (FWHM) of 10 fs. The peak intensity I_{H27} of the 27th harmonic pulse is fixed at 10^{13} W/cm^2, and we plot the results for five different values of fundamental peak intensity I_F indicated in the figure. Note that the wavelength of the 27th harmonic varies with that of the fundamental pulse.

He^+ for the case of simultaneous fundamental and an H27 irradiation with $\lambda_F = 800$ nm. We can see that the 2*s* level is in fact populated through two-color two-photon excitation and that about 8% of electron population is left in this level after the pulse while the 2*p* level is hardly excited. Since the 2*s* level lies only 13.6 eV below the ionization threshold, the electron can now be lifted to the continuum by the fundamental laser pulse much more easily than from the ground state and subsequently emit a harmonic photon upon recombination. Thus the ionization yield as well as the harmonic photoemission efficiency is largely increased. In order to check quantitatively whether this is true or not, we have calculated the harmonic spectrum from the superposition of

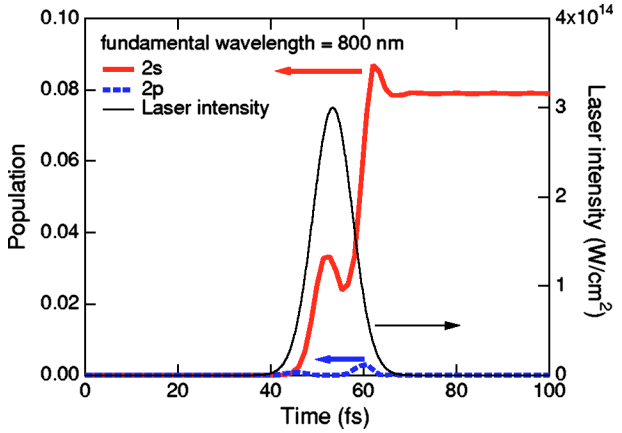

FIG. 10. (Color online) Temporal evolution of the 2*s* (thick solid) and 2*p* (thick dashed) population of He^+ exposed to a Gaussian combined fundamental and its 27th harmonic pulse with a duration (FWHM) of 10 fs, the former with a peak intensity of 3×10^{14} W/cm^2 and the latter 10^{13} W/cm^2. The fundamental wavelength is 800 nm. The thin solid line (the right axis) is the temporal profile of laser intensity.

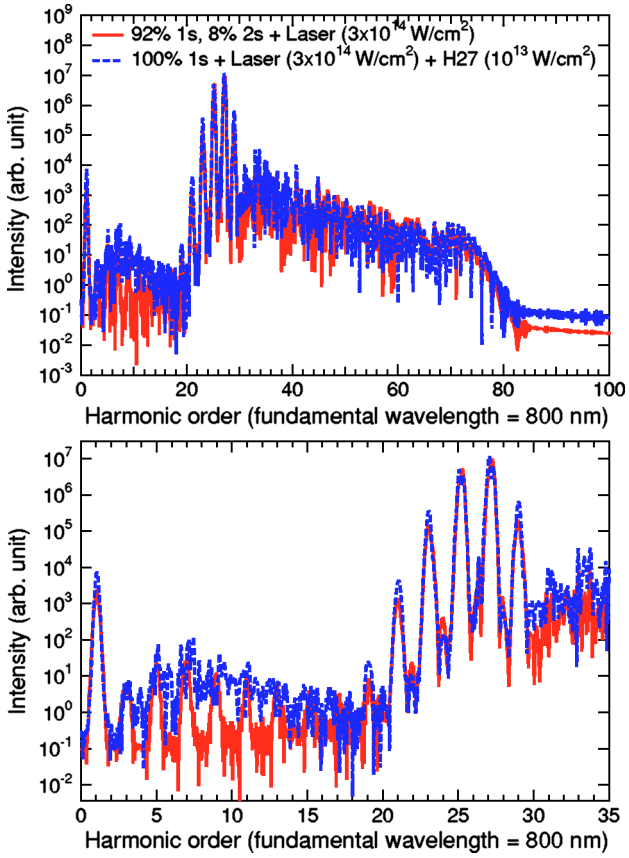

FIG. 11. (Color online) Solid curve: harmonic spectrum from the superposition of the 1*s* (92%) and 2*s* (8%) states of He^+ exposed to a fundamental laser pulse with a peak intensity of 3×10^{14} W/cm^2. Dotted curve: harmonic spectrum from the ground-state He^+ exposed to a combined fundamental and its 27th harmonic pulse, the former with a peak intensity of 3×10^{14} W/cm^2 and the latter 10^{13} W/cm^2. The fundamental wavelength is 800 nm. The two curves overlap each other in most parts. The bottom graph is a magnified view.

the 1*s* (92%) and 2*s* (8%) states subject to the laser pulse alone. The result is displayed in Fig. 11 along with the spectrum from the ground-state He^+ subject to the combined pulse. The two spectra are strikingly similar to each other both in peak heights and positions. Hence the enhancement mechanism for this case may also be interpreted as harmonic generation from a coherent superposition of states. Such a process has already been studied by Watson *et al.* [36]. They have found that the harmonic spectrum from a superposition of states consists of two distinct sets of harmonics: the first (lowest energy) plateau has a cutoff at $I_e + 3.17U_p$ with I_e being the ionization potential of the excited state, and the second plateau has a cutoff given by Eq. (3). They have reported that the spectrum does not depend on the initial relative phase between the states, which may partially explain our results in Fig. 3 that our spectrum is insensitive to the relative phase ϕ. They have also shown that the first and the second plateau efficiency scales as β^4 and $\alpha^2\beta^2$, respectively, where α and β denote the amplitudes of the ground and the excited states. In the case of the present study, the excitation of the 2*s* state is linear in I_{H27}, thus $\beta^2 \propto I_{H27}$, and

we can assume that $\alpha \approx 1$. Hence we expect that the first plateau scales as I_{H27}^2 and the second as I_{H27}. These results are consistent with the observations in Figs. 1 and 5, which reinforces our view that the enhancement at $\lambda_F = 800$ nm, $I_F = 3 \times 10^{14}$ W/cm^2, and $I_{H27} = 10^{13}$ W/cm^2 is essentially due to harmonic generation from a superposition of states. It is noteworthy that the H27 addition provides a means to prepare such a superposition, which was not explained in Ref. [36].

At $I_F = 3 \times 10^{14}$ W/cm^2, we can also see a third peak around $\lambda_F = 770$ nm corresponding to two-color $2p$ excitation involving one H27 and two fundamental photons. On the other hand, at $\lambda_F = 785$ nm, located between the second and the third peaks, we expect that there is very little excitation of the $2s$ and $2p$ states, though these are broadened by the dynamic Stark effect. Nevertheless the photoemission is still strongly enhanced, as we have seen in Fig. 4. The He^{2+} yield (0.046) is also much higher than in the case of the fundamental pulse alone (5.2×10^{-15}). In this case the population of $2s$ and $2p$ states after the pulse is 1.0×10^{-4} and 7.7×10^{-6}, respectively, and the other excited levels are virtually unpopulated. We have calculated the harmonic spectrum from the superposition of the $2s$ (1.0×10^{-2}%), $2p$ (7.7×10^{-4}%), and $1s$ states subject to the laser pulse alone with $\lambda_F = 785$ nm. The result is shown in Fig. 12 along with the spectrum from the ground-state He^+ subject to the combined pulse. In contrast to the case of $\lambda_F = 800$ nm (Fig. 11), the harmonic spectrum from the superposition cannot account for the primary peaks in the spectrum by the combined pulse. The results in Fig. 12 indicate that the electron is lifted to the continuum directly from the ground state and that the photoemission process can be viewed as two-color frequency mixing, enhanced by the fact that $\hbar\omega_{H27} - \hbar\omega_F$ and $\hbar\omega_{H27} - 2\hbar\omega_F$ are close to the resonance with $1s$-$2s$ and $1s$-$2p$ transitions, respectively. From this mechanism we expect the main plateau efficiency scaling as I_{H27} and weak photoemission at lower orders, consistent with the results presented in Figs. 4 and 6. The mechanism may also be interpreted as follows. A single H27 photon, in cooperation with one and two fundamental photons, promotes a transition to virtual states near the $2s$ and $2p$ levels. The electron can be lifted from these virtual states to the continuum by the fundamental pulse much more easily than from the ground state. The transition to the virtual states are facilitated since they lie near the intermediate ($2s$ and $2p$) levels, and, as a consequence, ionization and HHG efficiency are largely augmented. It should be noted in Fig. 12, however, that the spectrum from the ground state by the combined pulse contains small peaks which clearly correspond to those in the spectrum from the superposition by the fundamental pulse. This observation implies that both enhancement mechanisms of harmonic generation from a coherent superposition of states and two-color frequency mixing coexist in general and that their relative importance depends on fundamental wavelength. In both mechanisms, the entire process involves a single H27 photon. Hence, we expect that ionization yield is linear in the intensity of the H27 pulse irrespective of fundamental wavelength, as we have seen in Fig. 7.

Let us now return to the discussion in Fig. 9. The dynamic Stark effect induces not only the peak shift but also the peak broadening, which results in the decrease of peak heights at higher fundamental intensity. For example, the peak at $\lambda_F = 800$ nm is lower at $I_F = 5 \times 10^{14}$ W/cm^2 than at $I_F = 3 \times 10^{14}$ W/cm^2 and cannot be recognized anymore at $I_F = 10^{15}$ W/cm^2 due to too much broadening. This leads to the decrease of ionization yield at $I_F > 3 \times 10^{14}$ W/cm^2 in Fig. 8.

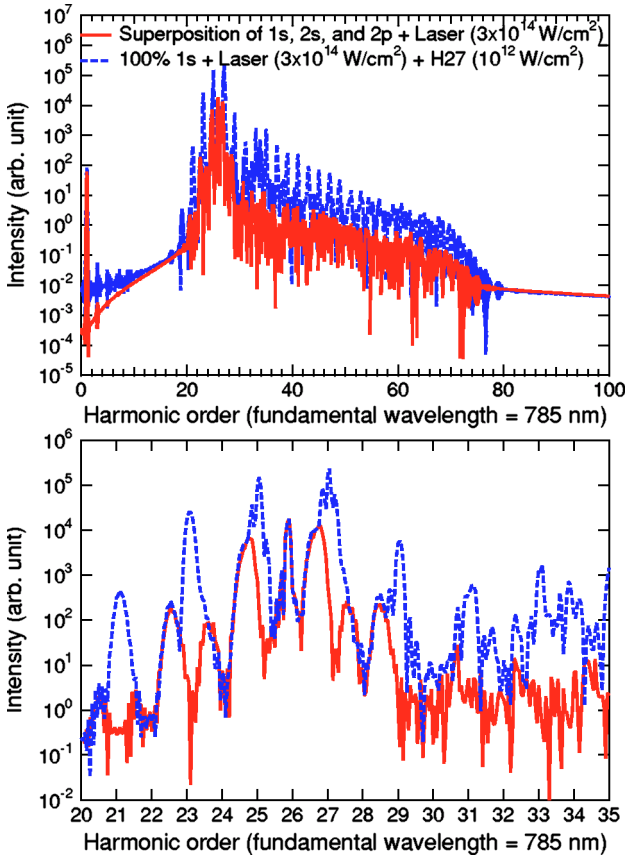

FIG. 12. (Color online) Solid curve: harmonic spectrum from the superposition of the $1s$, $2s$, and $2p$ states of He^+, as described in the text, exposed to a fundamental laser pulse with a peak intensity of 3×10^{14} W/cm^2. Dotted curve: harmonic spectrum from the ground-state He^+ exposed to a combined fundamental and its 27th harmonic pulse, the former with a peak intensity of 3×10^{14} W/cm^2 and the latter 10^{12} W/cm^2. The fundamental wavelength is 785 nm. The bottom graph is a magnified view.

Thus, the role of the fundamental laser pulse is three-fold: to assist transitions from the ground state to the $2s$ and $2p$ levels or virtual states near them through two-color excitation, to lift the electron from an excited (real or virtual) level to the continuum through optical-field ionization, and to induce dynamic Stark shift and broadening. The interplay of these three leads to a complicated behavior seen in Figs. 8 and 9.

Although we have mainly concentrated ourselves on the case of a combined fundamental and H27 pulse in the present section, a similar discussion applies to the case of the H13 addition. For this case, since twice the H13 photon energy is close to the $1s$-$2s$ and -$2p$ transition energy, primary ionization and photoemission channels involve two H13 photons, whether the underlying mechanism may be harmonic generation from a coherent superposition of states or two-

color frequency mixing. Hence we expect that the main plateau efficiency and the He^{2+} yield scale as I_{H13}^2 with I_{H13} being the H13 peak intensity, which can be confirmed in Figs. 2 and 7.

V. CONCLUSIONS

Using numerical simulations, we have investigated the photoemission and ionization behavior of a He^+ ion subject to a combined field of an ultrashort intense Ti:sapphire laser and its high-order harmonic pulses. Specifically we have considered the 27th and 13th harmonics, for which especially high intensity can be achieved with the state-of-the-art HHG technique. The response of He^+ is totally different from that in the case of the irradiation of the fundamental pulse alone or the harmonic pulse alone. The H27 addition enhances high-order harmonic photoemission even by 17 orders of magnitude, and the H13 addition also increases photoemission efficiency by more than ten orders of magnitude. Moreover, while an individual laser (λ_F=800 nm) or its 27th harmonic pulse with a peak intensity of 3×10^{14} and 10^{13} W/cm^2, respectively, ionizes no more than 5×10^{-6} of He^+, the combined pulse leads to a high He^{2+} yield of 17%.

Such enhancement is caused by two-color-field-induced transition to 2*p* and 2*s* states or to a nearby virtual state, which lie significantly closer to the ionization threshold than the ground state. When the real excitation of 2*p* and 2*s* states is present, the enhancement mechanism is harmonic generation from a coherent superposition of states. Otherwise the process can be viewed as two-color frequency mixing enhanced by the presence of a near-resonant intermediate level. In general the two mechanisms coexist, and their relative importance depends on fundamental wavelength: the former is dominant at λ_F=800 nm and the latter at λ_F=785 nm when a H27 pulse is added to a laser pulse with $I_F=3\times10^{14}$ W/cm^2. The harmonic pulse plays an essential role in transition to 2*p* and 2*s* states or to a nearby virtual state, and the fundamental pulse is important in OFI from these levels as well as in 1*s*-2*p*, 2*s* transitions through two-color excitation; their co-presence leads to the enhancement of both harmonic photoemission intensity and He^{2+} yield. Our results show that even a simple hydrogenlike system exhibits unexpected properties under appropriate perturbation. Although several issues such as production of fully ionized He^+ plasma and phase matching are yet to be resolved with regard to experimental implementation, the efficient H27- or H13-assisted harmonic generation might open a way to develop an intense light source of an even shorter wavelength than available today.

ACKNOWLEDGMENTS

We would like to thank E. J. Takahashi, K. Midorikawa, Y. Nabekawa, and H. Hasegawa for helpful discussions especially on experimental feasibility. We gratefully acknowledge fruitful discussions with P. Salières and A. de Bohan on the enhancement mechanism. This work has been partially supported by the Ministry of Education, Culture, Sports, Science and Technology of Japan, Grant No. 15035203.

[1] A. McPherson, G. Gibson, H. Jara, U. Johann, T. S. Luk, I. A. McInstyre, K. Boyer, and C. K. Rhodes, J. Opt. Soc. Am. B **4**, 595 (1987).
[2] M. Ferray, A. L'Huillier, X. F. Li, L. A. Lompré, G. Mainfray, and C. Manus, J. Phys. B **21**, L31 (1988).
[3] E. Takahashi, Y. Nabekawa, T. Otsuka, M. Obara, and K. Midorikawa, Phys. Rev. A **66**, 021802 (2002).
[4] E. Takahashi, Y. Nabekawa, and K. Midorikawa, Opt. Lett. **27**, 1920 (2002).
[5] E. Takahashi, M. Nurhuda, Y. Nabekawa, and K. Midorikawa, J. Opt. Soc. Am. B **20**, 158 (2003)
[6] V. Tosa, E. Takahashi, Y. Nabekawa, and K. Midorikawa, Phys. Rev. A **67**, 063817 (2003).
[7] E. Takahashi, V. Tosa, Y. Nabekawa, and K. Midorikawa: Phys. Rev. A **68**, 023808 (2003).
[8] E. J. Takahashi, Y. Nabekawa, and K. Midorikawa, Appl. Phys. Lett. **84**, 4 (2004).
[9] J.-F. Hergott, M. Kovacev, H. Merdji, C. Hubert, Y. Mairesse, E. Jean, P. Breger, P. Agostini, B. Carré, and P. Salières, Phys. Rev. A **66**, 021801 (2002).
[10] D. Yoshitomi, T. Shimizu, T. Sekikawa, and S. Watanabe, Opt. Lett. **27**, 2170 (2002).
[11] E. J. Takahashi, H. Hasegawa, Y. Nabekawa, and K. Midorikawa, Opt. Lett. **29**, 507 (2004).
[12] H. Mashiko, A. Suda, and K. Midorikawa, Opt. Lett. (to be published).
[13] Y. Kobayashi, T. Sekikawa, Y. Nabekawa, and S. Watanabe, Opt. Lett. **23**, 64 (1998).
[14] Y. Kobayashi, T. Ohno, T. Sekikawa, Y. Nabekawa, and S. Watanabe, Appl. Phys. B: Lasers Opt. **70**, 389 (2000).
[15] D. Descamps, L. Roos, C. Delfin, A. L'Huillier, and C.-G. Wahlström, Phys. Rev. A **64**, 031404 (2001).
[16] K. Ishikawa and K. Midorikawa Phys. Rev. A **65**, 043405 (2002).
[17] T. Nakajima and L. A. A. Nikolopoulos, Phys. Rev. A **66**, 041402 (2002).
[18] P. Salières, L. Le Deroff, T. Auguste, P. Monot, P. d'Oliveira, D. Campo, J.-F. Hergott, H. Merdji, and B. Carré, Phys. Rev. Lett. **83**, 5483 (1999).
[19] M. Hentschel, R. Kienberger, Ch. Spielmann, G. A. Reider, N. Milosevic, T. Brabec, P. Corkum, U. Heinzmanns, M. Dreschers, and F. Krausz, Nature (London) **414**, 509 (2001).
[20] M. Protopapas, A. Sanpera, P. L. Knight, and K. Burnett, Phys. Rev. A **52**, R2527 1995).
[21] K. Ishikawa and K. Midorikawa, Phys. Rev. A **65**, 031403 (2002).
[22] M. G. Makris, L. A. A. Nikolopoulos, and P. Lambropoulos, Phys. Rev. A **66**, 053414 (2002).
[23] Z. Zeng, R. Li, Y. Cheng, W. Yu, and Z. Xu, Phys. Scr. **66**, 321 (2002).
[24] K. C. Kulander, K. J. Schafer, and J. L. Krause, in *Atoms in*

Intense Laser Fields, edited by M. Gavrila (Academic, New York 1992), pp. 247–300.
[25] K. Ishikawa, Phys. Rev. Lett. **91**, 043002 (2003).
[26] K. L. Ishikawa, Appl. Phys. B: Lasers Opt. **78**, 855 (2004).
[27] S. Watanabe, K. Kondo, Y. Nabekawa, A. Sagisaka, and Y. Kobayashi, Phys. Rev. Lett. **73**, 2692 (1994).
[28] J. L. Krause, K. J. Schafer, and K. C. Kulander, Phys. Rev. A **45**, 4998 (1992).
[29] P. B. Corkum, Phys. Rev. Lett. **71**, 1994 (1993).
[30] M. Lewenstein, P. Balcou, M. Y. Ivanov, A. LfHuillier, and P. B. Corkum, Phys. Rev. A **49**, 2117 (1994).
[31] C. Figueira de Morisson Faria, M. Dörr, W. Becker, and W. Sandner, Phys. Rev. A **60**, 1377 (1999), and references therein.
[32] B. Wang, X. Li, and P. Fu, Phys. Rev. A **62**, 063816 (2000).
[33] T. Mercouris and C. A. Nicolaides, J. Phys. B **33**, 4673 (2000).
[34] T. Mercouris and C. A. Nicolaides, Phys. Rev. A **63** 013411 (2001).
[35] T. Mercouris and C. A. Nicolaides, Phys. Rev. A **67**, 063403 (2003).
[36] J. B. Watson, A. Sanpera, X. Chen, and K. Burnett, Phys. Rev. A **53**, R1962 (1996).
[37] A. L'Huillier, L. A. Lompré, D. Normand, X. Tang, and P. Lambropoulos, J. Opt. Soc. Am. B **6**, 1790 (1989).